Available online at www.elixirpublishers.com (Elixir International Journal)

Geoscience

Elixir Geoscience 62 (2013) 17669-17676

ISSN: 2229-712X

The contribution of electrical resistivity and seismic refraction techniques to Site characterization and earthquake risk assessment, a case study: IKIA airport, Iran

Khalil Rezaei[a], Vahab Amiri[b] and Ali Beitollahi[c]

[a]Sedimentology, Kharazmi University, Tehran, Iran.

[b]Hydrogeology, Kharazmi University, Tehran, Iran.

[c]Building and Housing research center (BHRC), Tehran, Iran.

ARTICLE INFO

Article history:

Received: 9 July 2013;

Received in revised form:

20 August 2013;

Accepted: 4 September 2013;

Keywords

Electrical Resistivity,

Seismic Refraction,

Geological Assessment,

IKIA airport.

ABSTRACT

Geophysical investigations are increasingly applied to urban planning development for mapping and monitoring. Vertical electric sounding method and seismic refraction technique were used in Imam Khomeini International Airport (IKIA) Iran, in an attempt to define the subsurface structure, variation in thickness and strength of layers and also, determine the earthquake prone zones in the area. Distribution of electrical resistivity indicated that the study area can be divided into two parts of northern-southern or northeast-southwest. The fine grain silt, clay, marble and chalk deposits with low resistivity are created thick layers in southern and southwest parts of area. In depths 30, 50, 100 and 150 m we are faced to change in soil materials, in the other word change in layer composition mainly occurred at these depths. Also, the real and vast aquifer cannot be considered for this site and just local small mounding of groundwater in some positions such as northern part of area, in deep old alluvial deposits can be guessed. It seems that fault or discontinuity is passed from northwest to the southeast of the study area and is caused the change in geology and sedimentary conditions. According to Iranian Seismic Code (Standard 2800), most of the land around the airport are in class 2 and 3 and the future construction in this region will be required to comply with the standard design principles.

Introduction

Depicting geological contact has its own benefits such as producing geological map, determination of deep crustal structural, and mapping geological boundaries for engineering purpose (Dearman & Fookesf, 2002; Guterch et al, 1986; Ugalde & Morris, 2010). Common geophysical techniques applied for delineating geological contacts are gravity method, resistivity method and seismic refraction method (Green, 1976; Ali et al, 2012; Fuis et al, 1987).

The objectives of this study were accurate detection of surface and subsurface layers and geologic units, determine the depth to groundwater, sedimentology study of the region and determine the thickness of alluvial deposits, study of tectonic and associated complications such as faults, discontinuities, fractures and folding, and determine the depth of bed rock. For these aims, two common geophysical methods including VES and seismic refraction were used. Electrical resistivity is one of the most sensitive geophysical methods for monitoring changes of electrical properties in the subsurface. The resistivity of soils is dependent on saturation, porosity, permeability, ionic content of the pore fluids, and clay content (Chinedu and Ogah, 2013). The Vertical Electrical Sounding (VES) which is based on resistivity of media was used for this study because the instrumentation is simple, field logistics are easy and straight forward while the analysis of data is economical and less tedious (Ayolabi, 2005; Oladapo et al 2004; Olorunfemi et al 1999; Omosuyi et al 2008; Van Overmeeren, 1989 and Zohdy et al 1974).

Similar to the electrical resistivity, seismic refraction is one of the most commonly used methods to determine bedrock depths, especially for depths of less than 30 m (Telford et al 1990). This method which has been used in various and numerous studies (Dawood et al 2012; Imhof et al 2011; Nisa et al 2012; Williams et al 2005) is based on Snell's law. This law governs the refraction of sound or light ray across the boundary between layers of different physical properties. As sound waves travel from a medium of low seismic velocity into a medium of higher seismic velocity, some are refracted towards the lowers velocity medium and some are reflected back into the first medium. The refracted waves arrive at the earth's surface where it can be detected by a geophone which generates an electrical signal and sends the signal to a seismograph (Haeni, 1978).

The present paper mainly aims to show how the geophysical investigations can play a significant role in a characterization study of the geological structures in an area that is intended for future constructional operations. Their application can accelerate the study and easily spread out the results to wider areas. Although the paper is mainly focused on the analysis and the evaluation of the geophysical results, reference is also given to their incorporation in techniques for the seismic and earthquake risk assessment, in order to provide an integrated picture of the contribution of the geophysical surveys in the whole procedure.

Tele:

E-mail addresses: Khalil.Rezaei@yahoo.com

Materials And Methods

Theory of Applied Methods

Electrical Resistivity

In this part of investigation, the short description for resistivity method is presented because the fundamental theory behind this method was expanded and the theory has been adequately covered (Bhattacharya and Patra, 1968; Grant and West, 1965; Keller and Frischknecht, 1966).So, electrical prospecting makes use of a variety of principles, each based on some electrical properties or characteristics of the materials in the earth (Egbai and Asokhia, 1998). During resistivity surveys, current is injected into the earth through a pair of current electrodes, and the potential difference is measured between a pair of potential electrodes. The current and potential electrodes are generally arranged in a linear array. Common arrays include the dipole-dipole array, pole-pole array, Schlumberger array, and the Wenner array. The apparent resistivity is the bulk average resistivity of all soils and rock influencing the current. It is calculated by dividing the measured potential difference by the input current and multiplying by a geometric factor specific to the array being used and electrode spacing (Beck, 1993; Dobrin, 1976).

Seismic Refraction

The seismic refraction technique is based on the refraction of seismic energy at the interfaces between subsurface/ geological layers of different velocity (Dawood et al 2012). Seismic Refraction method uses seismic energy that returns to the surface after traveling through the ground along refracted ray paths. The first arrival of seismic energy to a detector offset from a seismic source always represents either a direct ray or a refracted ray (Reynolds, 1997).

The seismic refraction method uses very similar equipment to seismic reflection, typically utilizing geophones in an array, and a seismic source (shot) (Dawood et al 2012).When a seismic wave encounters an interface between two different rock types, some of the energy is reflected and the remainder continues on its way at a different angle, i.e., it is refracted (Dawood et al 2012; Gadallah and Fisher, 2004). Seismic refraction method is governed by Snell's law, which relates the angles of incidence and refraction to the seismic velocities in the two media (Dawood et al 2012).Further readings on seismic profiling could be seen from numrous works (Aki, 1969; Imhof et al 2011; Imhof et al 2011; Yilmaz, 1987).

Materials &Data Accusation

Electrical Resistivity Method

The electrical resistivity method employed in this study is the Schlumberger array configuration (Millitzer et al 1979; Mundri, 1980). In this method, measurements were made with increasing separation between the electrodes about the midpoint. The Schlumberger method was adopted for this study because of the fieldwork is faster, easier and economically save the money and software's are rapidly available for its interpretation (Selvam et al 2010; Todd, 1980).

In electrical resistivity measurements, the traditional four-electrode resistivity configurations as described in, Dobrin and Savit (1988) and Telford et al (1990), have been confirmed inadequate (Griffiths and Barker, 1993; Loke, 1999; Loke and Barker, 1995). Therefore in this study, the field procedure as described in Loke (1999) was adopted. The Schlumberger sounding were carried out in 6 profiles include 60 sounding stations (Fig.1) with current electrode spacing (AB) up to 928m. The distance used for potential electrode spacing (MN) was up to 30m. At each VES station electrodes were placed in a straight line and the inter-electrode spreads were gradually increased about a fixed center. The current was sent into the ground and the potential difference (**V**) due to this current was measured and recorded against the electrode spacing. With these values of currents (**I**) and potential (**V**) of the electrode configuration adopted one can get the apparent resistivity (ρ**a**). The apparent resistivity values were plotted against AB/2 on double-log graph sheets. The manner in which apparent resistivity values increase or decrease with electrode separation forms the basis for choosing the shape of the field curve that can perform quantitative interpretation of the sub surface resistivity distribution (Muthuraj et al 2010).

Seismic Refraction Method

In this study, a seismic equipment-set consist of a hammer for striking the shot-point (wave source), a high-speed digital data recording systems called seismographs (ADEN Terraloc MK8 24-channel seismograph), a seismic imager software (Seistw program) and acoustic sensors called geophones (30 Geophone (P) 10 HZ, 25 Geophone (P) 30 HZ, and 30 Geophone (S) 10 HZ) were used. The seismic refraction pulses were recorded for the forward and reverse shots.

The 24 seismic refraction profiles including 12 longitudinal wave profiles and 12 shear wave profiles were performed (Fig.1). In this site, for each P profile five shots and for each S profile six shots with shear wave sources and mutual reverse polarity are done.

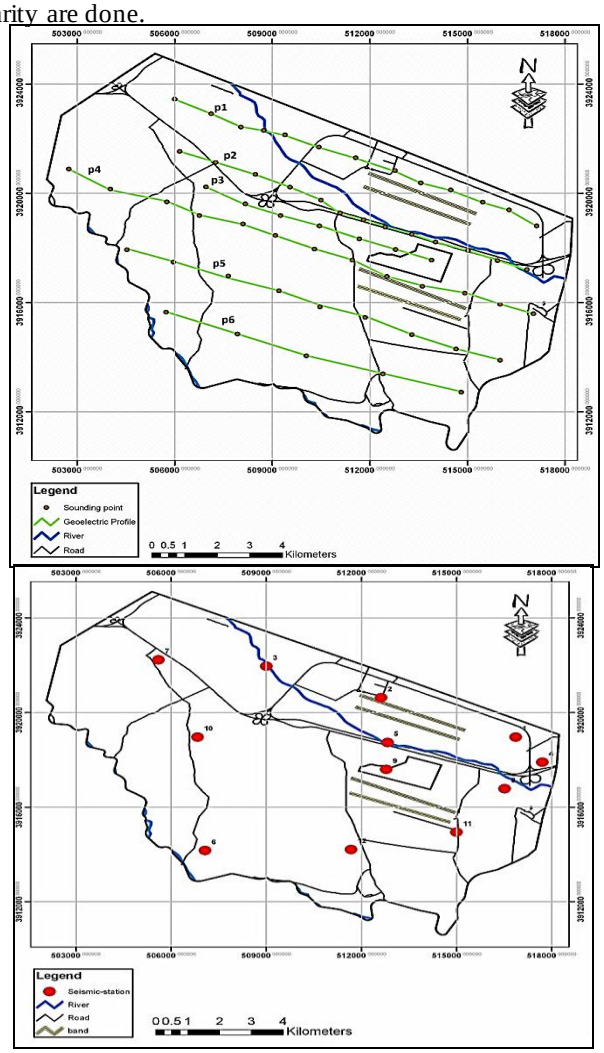

Fig.1. Position of geoelectrical (left) and seismic refraction profiles (right).

Site Description

The study area was Imam Khomeini International Airport (IKIA) and its environs, between longitudes 505000 to 518000 and latitudes 391400 to 392300. This site which has about 100 km^2 area is located about 30 kilometers (19 mi) southwest of the city of Tehran, near the localities of Robat-Karim and Eslamshahr. Based on hydrologic divisions, this area is the lowest parts of the Tehran basin and Robat-Karim, Shour rivers reach to this area in the end of their path. Morphologically, the study area composed of flat alluvial plain and low-lying hilly and the general topography slop is north to the south. Average slope angle of hills is approximately 20 to 40 degrees and for flat alluvial plain is generally between 5 to 10 degrees. Field observations show that the surficial sediments in the northern part of the area are mostly fine grain and loose sediments and in the south of area coarse grain and dense conglomerate layers can be observed. In this area, sediments have the poor and very poor sorting which fall in range from gravel to clay. Due to Robat-Karim fault, study area has the relatively high seismicity and risk potential.

Results And Discussion

As shown in figure 1, the 6 geoelectrical profiles include 60 sounding stations and 24 seismic refraction profiles include 12 longitudinal (P) wave profiles and 12 shear (S) wave profiles were used in this study.

The results of first part are presented as vertical electrical sounding curves displaying the geoelectrical parameters (layer resistivity, material type and thicknesses) and geo-structural maps. In this study, profile1 was performed in the north of active band of terminal1, profiles 2-4 were in center of area and between old and new bands, and profiles 5, 6 were implemented in the south of under construction bands of terminal 2.The field data were interpreted and processed qualitatively and quantitatively by using partial curve matching techniques and computer to obtain the resistivity values of different subsurface layers and their corresponding thickness. In table 1, summary of compute output of geoelectrical survey in IKIA site is presented.

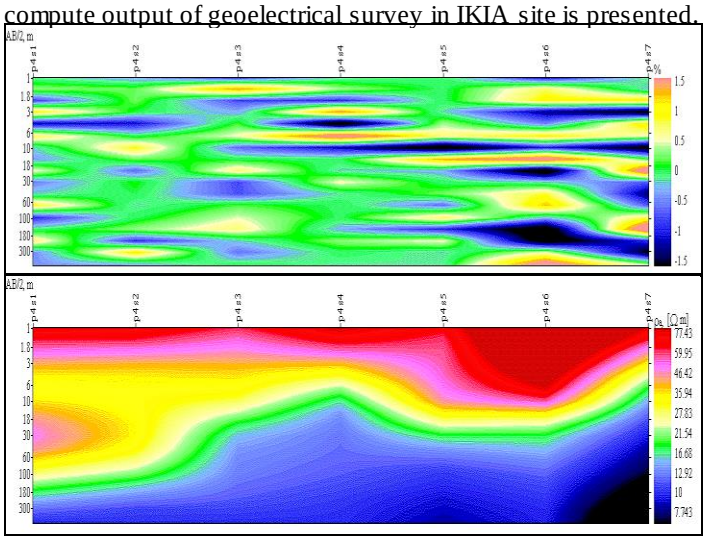

Fig.2. Distribution of fitting error (top) and geoelectrical pseudo-section (down) for eastern part of profile 4 (for example).

Preparing the geoelectrical pseudo-section for each profile was the first step of interpretation process. This work was done by smoothing the collected field data and drawing the contours of apparent electrical resistivity in different AB/2 measurements. This profile shows the distribution of apparent electrical resistivity (Fig.2) in depth and for different AB spaces.

In figure2, an example of geoelectrical pseudo-section for eastern part of profile 4 is presented. In addition, the distribution of fitting error for each profile showed the good process of field data. In general, the interpretation of VES curves depicted three layers within the study area. This claim is proved gradually in the next parts of study.

The geoelectrical pseudo-section for western part of profile 1 showed the high resistivity in S2, S3 (probably due to compact and coarse grain soil) which has continued to depth 150m; this layer has not seen in S1 and S7. Also, in S9, eastern part of profile 1, this coarse grain layer is has continued to depth 50 m. In this profile, bed rock is furnished by marble and has the low resistivity. In profile 2, S1, S4 and S5 showed the more thickness of high resistivity surface layer than other sounding points. The intermediate layer showed the low resistivity and thickness almost in all sounding positions. Recorded resistivity indicated the marble and clay bedrock for this part of profile. The VES data for eastern part showed the repetitious change of grain size in sounding points.

Profile 3 which was located in center of IKIA site specified the medium to coarse deposits for depth 3-40m. In this profile, the bedrock depth is gradually increased from west to east. The high electrical resistivity was recorded for S4 which probably is due to coarse grain sediments or an oblique discontinuity; of course the later guess is more close to real. Both part of profile 4 had a same trend by means that along this profile the medium to coarse sediments covered the underground media and S6, S7 (in eastern part) andS8, S9 (in western part) depicted shallow lenses of coarse and compact deposits.

In profile 5 (southern part of IKIA), S3, S4, S7 and S8 showed the high resistivity which is because of coarse grain sediments. Low resistivity of media proved the shallow bedrock for this profile. The main difference between northern and southern parts of IKIA site which is depth of bedrock and thickness of deposits was observed in this profile and next profile. The sharp change of bedrock depth along these profile spatially early one is the sign of fault effect in this region.

Interpretation of electrical resistivity for profile 6 is similar to previous one. The possible fault or discontinuity was unfolded between S2 and S3.

Although the electrical resistance is the basic parameter in geophysical exploration but, the estimated values of electrical conductivity (EC) can be used in hydro-geological studies. The electrical conductivity is the product of a complex process of water and substrate interaction (Heilan, 1940). In this study, analysis the change of electrical conductivity was performed for all profiles. Figure 3shows an example of model output for this part. Results showed that S4 in both profile 1 and 2 has the low EC and this illustrates the coarse grain sediments which can make the suitable condition for water accumulation. Profiles 2-6 showed more EC than profile 1 spatially eastern part (Table 1) and this is because of clay, chalk and marble sediment and existence of probable groundwater. Change of EC in each profile is inversely related to its resistivity variation.

In addition, based on electrical resistivity and EC values of all profiles, the real and vast aquifer cannot be considered for this site and just local small mounding of groundwater in some positions such as northern part of area, in deep old alluvial deposits can be guessed.

As shown in table1, various parts of each profile have the different range of apparent electrical resistivity. The distribution of apparent electrical resistivity recorded for eastern part of

profile 4 is presented in figure 3, for example. In VES method, the electrical resistivity values of all sounding point on a profile can be used for type curve detection. In fact, analysis the distribution of electrical resistivity in this study can leads to determine the type curve of each profile. So, based on this theory, Q-type curve can be detected for IKIA site.

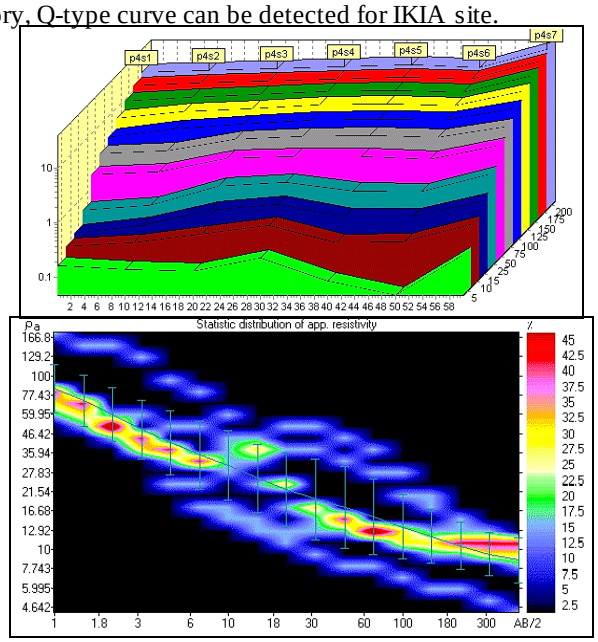

Fig.3. Computer output for change in electrical conductivity (left) and statistical distribution of apparent electrical resistivity (right) (first part of profile 4, for example)

In addition, the subsurface layer determination is one of the main applications of electrical resistivity distribution in each profile and/or sounding point. Therefore, the vertical and horizontal transformation of electrical resistivity (table 1) can play key role in subsurface layer detection. Results showed the periodic gradient of vertical transformation of electrical resistivity (VT) in sounding points which has the various soils at different depths. In general, the positive and negative values of VT were recorded in low and high depths of profiles, respectively. Almost in all profiles, VT showed the three subsurface layers with various depths in IKIA site. Horizontal transformation of electrical resistivity (HT) which can be used for discontinuity detection, horizontal change in alluvial properties and lithological variance in bedrock was performed in this site. The main use of HT data was in addressing the fault in study area. The HT profiles depicted a fault or discontinuity in profile 3 (between S1, S2), profile 4 (between S10, S11), profile 5 (between S2, S3 and S5, S6) and profile 6 (between S2, S3).

So, based on collected dada, three layers can be detected which as mentioned in some positions has the breakdown or displacement due to fault effect. The geological sections for 6 geoelectrical profile which are prepared by using all collected data by VES method are presented in figure 4.

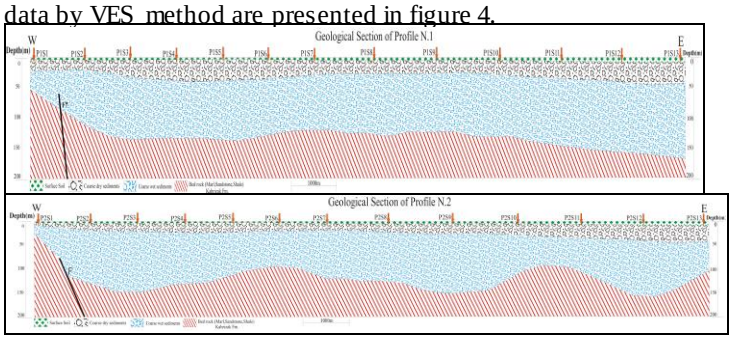

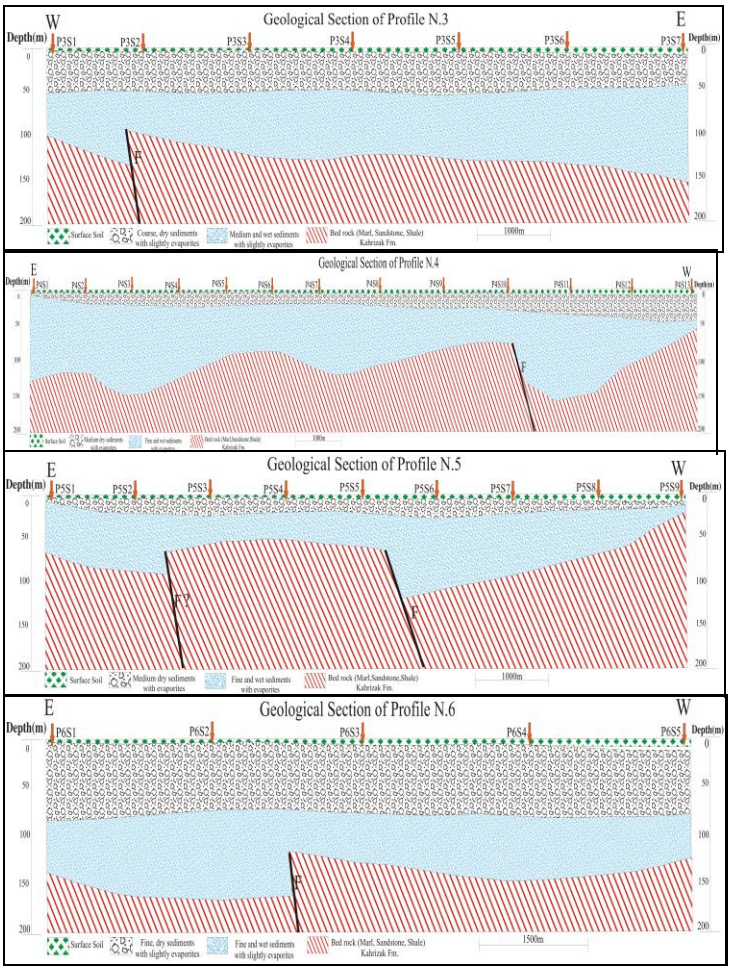

Fig.4. The geological sections of geoelectrical profiles

As shown in figure 4, three main layers which have the different thickness can be detected in IKIA site. Generally, in depths 30, 50, 100 and 150 m we are faced to change in soil material. The iso- resistivity maps for mentioned and key depths are showed in figure 5.

The prepared map for depth 30 m showed the range of 1-122Ωm for electrical resistivity fluctuation. In this depth, most points showed the resistance less than 25Ωm. In addition, the high recorded values of resistivity evidenced a close and coarse grain sedimentary basin in north part of site.

The iso- resistivity map for depth 50m illustrated the range 1-110Ωm for resistivity fluctuating and because of bedrock locating in this depth, the northern parts have higher resistivity of 50 Ωm. In depth 50 m, the most areas have resistivity value less than 20 Ωm.

In depth 100m, electrical resistivity decreased with increasing depth and varies between 1 and 77 Ωm. In this depth, most of underground media showed the low (less than 12 Ωm) resistivity.

Map of depth 150 m showed (Fig.5) the change in resistivity values between 1-60 Ωm and most positions had less than 12 Ωm. Although the bedrock of area in all domain has the same lithological formation, but it seems that there is a fault causing the separation of the two northern and southern regions.

In the study area, seismic refraction method along with VES has been used to investigate the depth of the subsurface layering and engineering characterization of geological materials. Seismic refraction data collected from the field were plotted in a time-distance graph, the compressional velocity; v_p and shear

velocity; v_s of the various zones measured on whole profiles were recorded as shown in table 1.

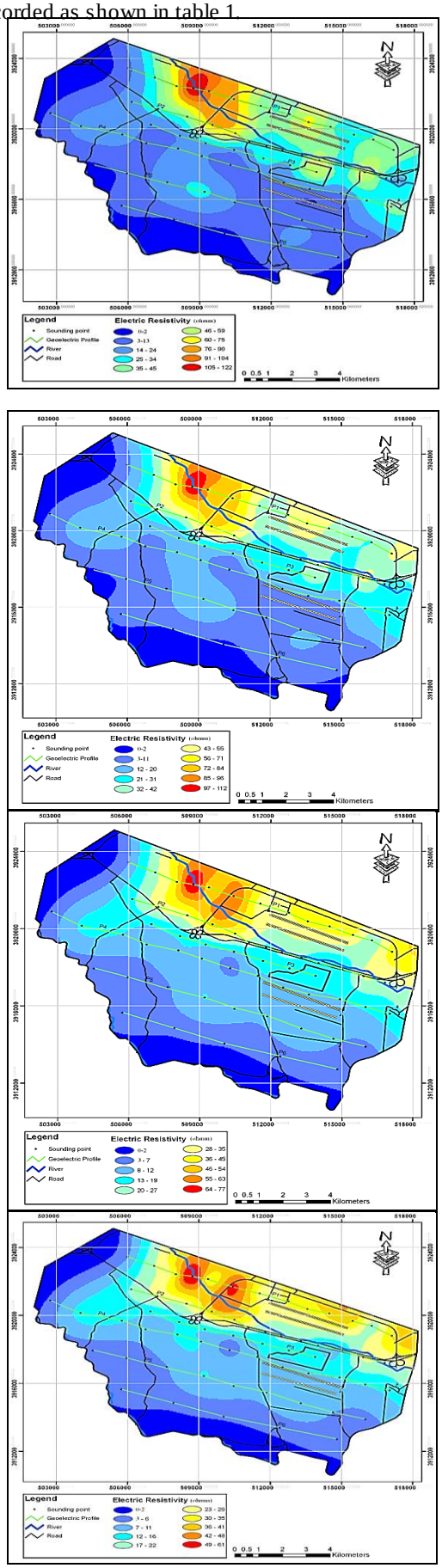

Fig.5.Iso-resistivity maps for depth30m (top-left), 50m (top-right), 100m (down-left) and 150m (down-right)

Similar to VES, results showed the three layers with different P and S wave velocities and consequently thickness and Poisson's ratios in IKIA site (Table 2, 3). In seismic method, the depth or thickness of each layer earth can be obtained by taking the average velocities of the forward and reverse curves and the intercept time.

Based on seismic P wave velocity records for IKIA site (Table 2), the first layer in the central area of Terminal 2 and West of site has the high velocity which is over 900 m/s while in the north, south, and east is reduced to about 300 to 400 m/s. Low velocity shows weakness and lack of soil stability in north, south and east Airport site. Also in second layer, the northeast and southwest of site are shown the low velocities, and center and northwest of the site are shown the high velocities for compressional (P) wave. The second layer has a higher velocity values than first layer. It seems that most chosen positions for band and second terminal did not have a problem. The third layer shows the same trend as the second layer to the P wave. Based on the recorded seismic P waves for second layer, some of active terminal bonds have not suitable condition and are constructed on weak and loose lands.

According to seismic S wave velocity records for IKIA site (Table2), the first layer shows the high velocity (more than 400 m/s) in central area of terminal 2 and west of site, and very low values (less than 200 m/s) is recorded for north and south of the site. Areas with low velocities are composed of loose and weak compaction which construction planes in these areas will be required to comply the standard design principles. In the second and third separated layers, the zones with low and high seismic shear (S) wave velocity is approximately equal, and northeast and southwest of the airport site has the low velocities, in addition to containing loose soils, highly weathered stones, and low depth to groundwater. Therefore, the engineering condition of these areas should be more considered during the construction operations. Based on average seismic S wave velocity map, the north and south lands of the airport have the velocity faster than 420 m/s, and is composed of loose and inappropriate formations (earth type 3 and 4). In addition, the center and northwest lands of the airport site are very strength and according to Iranian Seismic Code (Standard 2800) are first class.

Calculation of thickness for each layer by seismic refraction technique (Table 3) showed that the maximum value (up to 11 m) can be addressed in north and south of area and minimum thickness (1 to 3 m) is available in west and east of this site. For second layer, maximum (17 to 19 m) and minimum (7 to 8 m) thickness can be observed in south and northwest, and west and east of area, respectively. At the northeast and southwest of the area, seismic bedrock is in the deepest state (about 22 to 24 meters), and at the northwest of the airport site is located about 13 meters. Of course, the seismic bedrock is not equal to geology bedrock, it seems that high compaction of coarse-grained alluvial sediments has been cause the making of seismic bedrock.

Seismic method indicated that Poisson's ratio (Table 3) for the first layer is in rang of 0.28 to 0.4, and this value is gradually increases from east to west of site. The east of airport site shows the lowest and southwest and north of active terminal bands has the highest Poisson's values. According to Poisson's ratio, the first layer is composed of sand with medium density (Braja, 2008), so, most parts of this site are suitable for future engineering constructions.

Table1. Summary of VES data interpretations

Profile No.	Position	Part/Direction	ρ(Ωm) (≈)	HT[1]	VT[2]	Max. log EC[3] (≈)	Max. Fitting Error%
1	S1-S7	Western	6-167	-7.5-7.5	-20-20	15	2
	S7-S13	Eastern	22-72	-3-3	-15-15	2	1
2	S1-S7	Western	16-316	-15-15	-20-20	10	1.5
	S7-S13	Eastern	14-47	-7.5-7.5	-20-20	10	1.5
3	S1-S7	W-E	10-100	-20-20	-30-30	10	2
4	S1-S7	Eastern	7-75	-4-4	-20-20	10	1.5
	S7-S13	Western	5-140	-10-10	-30-30	20	2.25
5	S1-S9	E-W	5-100	-10-10	-30-30	15	2.5
6	S1-S5	E-W	1-15	-1-1	-20-20	100	1.75

[1] Horizontal transformation of electrical resistivity
[2] Vertical transformation of electrical resistivity
[3] Electrical Conductivity

Table 2. Values of P and S wave velocity for all layers

Profile No.	X(m)	Y(m)	First layer		Second layer		Third layer		v_s (Ave. to 30 m)
			v_p(m/s)	v_s(m/s)	v_p(m/s)	v_s(m/s)	v_p(m/s)	v_s(m/s)	
1	516864	3918967	650	300	950	500	1150	630	424
2	512626	3920627	550	260	750	400	900	490	370
3	509004	3921954	600	270	1650	940	2600	1520	705
4	517711	3917899	550	250	950	550	1200	700	466
5	512826	3918739	800	360	1500	680	1750	800	696
6	509528	3920174	500	235	800	460	1050	620	390
7	505599	3922227	850	390	1350	780	1550	910	765
8	516513	3916781	550	260	1150	590	1600	820	443
9	512791	3917596	950	460	1400	750	1650	940	706
10	506829	3918967	800	350	1100	630	1300	780	573
11	515002	3914942	750	360	1150	660	1400	820	643
12	511675	3914209	500	250	1450	670	2250	830	476

Table 3. Values of Poisson's ratio and thickness for all layers

Profile No.	X(m)	Y(m)	First layer		Second layer		Third layer	
			Z(m)	Poisson' ratio	Z(m)	Poisson' ratio	Z (m)	Poisson' ratio
1	516864	3918967	-10.5	0.36	-11.5	0.31	-22	0.29
2	512626	3920627	-7	0.36	-15.5	0.3	-22.5	0.29
3	509004	3921954	-6.5	0.37	-7.5	0.26	-14	0.24
4	517711	3917899	-6.5	0.3	-12.5	0.25	-19	0.35
5	512826	3918739	-2	0.37	-11.5	0.37	-13.5	0.23
6	509528	3920174	-8.5	0.36	-11	0.25	-19.5	0.24
7	505599	3922227	-2.5	0.37	-14	0.25	-16.5	0.32
8	516513	3916781	-9.5	0.36	-13	0.32	-22.5	0.26
9	512791	3917596	-6.5	0.35	-12.5	0.3	-19	0.22
10	506829	3918967	-5.5	0.38	-17	0.26	-22.5	0.22
11	515002	3914942	-3.5	0.35	-15.5	0.25	-19	0.24
12	511675	3914209	-8.5	0.33	-11	0.36	-19.5	0.42

Poisson's ratio of the second layer has changed in range 0.22 to 0.37 (loose sands) and just central parts and terminals 1, 2 are showed higher values and lowest Poisson's ratio was recorded for east and west of site. In third layer, the Poisson's ratio was between 0.18 to 0.43 which show the vast range of particle size from sand and gravel, silty sand and dens sand (Braja, 2008).

Conclusion

Results of site characterization and geological assessment in Imam Khomeini International Airport (IKIA) based on VES and seismic refraction surveys can be expressed as follows:

The fine grain chalk, marble and clay deposits with low resistivity are created thick layers in southern and southwest parts of area.

Distribution of electrical resistivity indicated that the study area can be divided into two parts of northern-southern or northeast-southwest.

Results showed that S4 in both profile 1 and 2 has the low EC and this illustrates the coarse grain sediments which can make the suitable condition for water accumulation. Profiles 2-6 showed more EC than profile 1 spatially eastern part and this is because of clay, chalk and marble sediment and existence of probable groundwater.

The main difference between northern and southern parts of IKIA site which is depth of bedrock and thickness of deposits was observed in profile 5, 6.

Results showed the periodic gradient of vertical transformation of electrical resistivity (VT) in sounding points which has the various soils at different depths. In general, the positive and negative values of VT were recorded in low and high depths of profiles, respectively. Almost in all profiles, VT showed the three subsurface layers with various depths in IKIA site.

Horizontal transformation of electrical resistivity (HT) which can be used for discontinuity detection, horizontal change

in alluvial properties and lithological variance in bedrock was performed in this site. The main use of HT data was in addressing the fault in study area. The HT profiles depicted a fault or discontinuity in profile 3 (between S1, S2), profile 4 (between S10, S11), profile 5 (between S2, S3 and S5, S6) and profile 6 (between S2, S3).

Based on electrical resistivity and EC values of all profiles, the real and vast aquifer cannot be considered for this site and just local small mounding of groundwater in some positions such as northern part of area, in deep old alluvial deposits can be guessed.

Based on seismic refraction studies, three layers are separable which with increasing in depth the S and P wave velocity is added and this indicates increasing in compaction of geology formations.

In the second and third separated layers, the zones with low and high seismic shear (S) wave velocity is approximately equal, and northeast and southwest of the airport site has the low velocities, in addition to containing loose soils, highly weathered stones, and low depth to groundwater. Therefore, the engineering condition of these areas should be more considered during the construction operations.

Based on average seismic S wave velocity map, the north and south lands of the airport have the velocity faster than 420 m/s, and is composed of loos and inappropriate formations (earth type 3 and 4). In addition, the center and northwest lands of the airport site are very strength and according to Iranian Seismic Code (Standard 2800) are first class.

The Poisson's ratio indicated that the most important and key installations of airport site are located in suitable positions.

At the northeast and southwest of the area, seismic bedrock is in the deepest state (about 22 to 24 meters), and at the northwest of the airport site is located about 13 meters. Of course, the seismic bedrock is not equal to geology bedrock, it seems that high compaction of coarse-grained alluvial sediments has been cause the making of seismic bedrock.

According to Iranian Seismic Code (Standard 2800), most of the land around the airport are class 2 and 3 and the future construction in this region will be required to comply with the standard design principles.

Like the VES results, it seems that a fault or a discontinuity is passed from northwest to the southeast of the study area and is caused the change in geology and sedimentary conditions.

References

1. Aki, K. 1969 .Analysis of the seismic code of local earthquakes as scattered waves: J,Geophysics Res., 74, 615-631.

2. Ali, N., Saad, R., Nordiana, M.M., Ismail, N.A., Ismail, N.E.H., Andy, A.B. and TehSaufia, A.H.A. 2012. Locating Contact Zone and Faults Utilizing Resistivity Method. International Conference on Arts, Social Sciences and Technology, Penang, Malaysia.

3. Ayolabi, E.A. 2005. Geoelectric elevation of groundwater potential: A case study of Alagba Primary School, Akure south-west Nigeria, Journal of Geological society of India, 66 pp 491-495.

4. Beck, A.E. 1993. Physical Principles of Exploration Methods. Wuerz Publishing Ltd, Canada; 2Rev Ed edition. 292 pp.

5. Bhattacharya, P.K. and Patra, H.P. 1968: Direct Current geoelectric sounding. Elsevier, Amsterdam. 135pp.

6. Braja, M.D. 2008. Advanced soil mechanics.3rd edition. Routledge Publication. ISBN: 0415420261, 9780415420266. 567 pp.

7. Chinedu, A.D. and Ogah, A.J. 2013. Electrical Resistivity Imaging of Suspected Seepage Channels in an Earthen Dam in Zaria, North-Western Nigeria.Open Journal of Applied Sciences, 3, 145-154

8. Dawood, A.M.A, Akiti, T.T. and Glover, E.T. 2012. Seismic Refraction Investigation at a Radioactive Waste Disposal Site. Geosciences, 2(2): 7-13, DOI:10.5923/j.geo.20120202.02

9. Dearman, W.R. and Fookesf, P.G. 2002. Engineering Geological Mapping For Civil Engineering Practice In The United Kingdom. Mapping In Engineering Geology, 1: 79-112.

10. Dobrin, M.B. 1976, Introduction to geophysical prospecting. McGraw-Hill Book Co, 630 pp.

11. Dobrin, M.B. and Savit, F. 1988. Introduction to Geophysical Prospecting. McGraw-Hill Company Ltd., NewYork.

12. Egbai, J.C. and Asokhia, M.B. 1998. Correlation between Resistivity survey and well- logging in DeltaState, Nigeria. JNAMP, 2: 163-175.

13. Fuis, G., Zucca, J., Mooney, W.D. and Milkereit, B. 1987. A geologic interpretation of seismic-refraction results in northeastern California. Bulletin of the Geological Society of America, 98 (1): 53.

14. Gadallah, M.R. and Fisher, R.L. 2004. Applied Seismology. PennWell Books.473 pp

15. Grant, F.S. and West, O.F. 1965: Interpretation theory inapplied geophysics. McGraw-Hill, New York, 583 pp.

16. Green, R. 1976. Accurate Determination of the Dip Angle of a Geological Contact Using the Gravity Method. Geophysical Prospecting, 24(2): 265-272.

17. Griffiths, D.H. and Barker, R.D. 1993. Two-Dimensional Resistivity Imaging and Modeling in Areas of Complex Geology. Journal of Applied Geophysics, Vol. 29, No. 3-4, pp. 211-226. doi:10.1016/0926-9851(93)90005-J.

18. Guterch, A., Grad, M., Materzok, R. and Perchuc E. 1986. Deep structure of the Earth's crust in the contact zone of the Palaeozoic and Precambrian platforms in Poland (Tornquist-Teisseyre Zone). Tectonophysics, 128(3-4): 251-279.

19. Haeni, F.P. 1978. Computer modeling in ground water availability in the Pootatuck River Valley, Newton,Connecticut with a section on quality water by Elinor H.H U.S geological survey. Water resourcesinvestigations, pp: 77-78.

20. Heilan, C. A. 1940. Geophysical exploration. Prentice Hall, NewYork, N.Y.

21. Imhof, A.L.; Sanchez, M.; Calvo, C. and Martin, A. 2011. Application of seismic refraction tomography for tunnel design in Santa Clara Mountain, San Juan, Argentina. Earth Sci. Res. J., vol.15, n.2, pp. 81-88. ISSN 1794-6190.

22. Iranian code of practice for seismic resistance design of buildings: Standard no.2800, 3rd edition. 2005. Building and Housing Research Center (in Persian).

23. Kearey, P., Brooks, M. and and Hill, I. 2009. An Introduction to Geophysical Exploration, Third Edition. Wiley Pub. New York, 272 pp.

24. Keller, G.V and Frischknecht, F.C. 1966: Electrical methods in geophysical prospecting. Pergamon, oxford. 517 pp.

25. Loke, M.H. 1999. Electrical Imaging Surveys for Environment and Engineering Studies (A Practical Guide to 2D and 3D Surveys). Earth Sciences, Vol. 6574525, No. 1999.

26. Loke, M.H. and R Barker, D. 1995. Least-Squares Deconvolution of Apparent Resistivity Pseudosections. Geophysics, Vol. 60, No. 6, pp. 1682-1690.
27. Millitzer, h., roster, r. and losch, w. 1979. Theoretical and experimental investigations for cavity research with geoelectrical resistivity methods. Geophysical Prospecting, 27, 640-652.
28. Mundri, e. 1980. The effect of a finite distance between potential electrodes on Schlumberger resistivity measurement-A simple correction graph. Geophysics, 45 (12), 1872-1875.
29. Muthuraj D., SrinivasY. and Chandrasekar N. 2010. Delineation of groundwater potential areas - a Case study from Tirunelveli District, TamilNadu, India, International journal of applied environmental sciences, 5, pp 49-56.
30. Nisa, A., Rosli, S., Saidin, M.M and Nordiana, M.M. 2012. Applying Seismic Refraction Method in Depicting Geological Contact at Bukit Bunuh, Lenggong, Perak, Malaysia. International Conference on Geological and Environmental Sciences, IPCBEE vol.3 6, IACSIT Press, Singapoore
31. Oladapo, M.I., Mohammed, M.Z., Adeoye, O.O. and Adetola, B.A. 2004. Geoelectrical investigation of the Ondo State Housing Cooperation Estate, IjapoAkure, Nigeria. J. of mining and geology 40 (1), pp. 41- 48
32. Olorunfemi, M.O., Ojo, J.S. and Akintunde O.M. 1999. Hydro-geophysical evaluation of groundwater potentials of Akure metropolis, Southern Nigeria J. Mining and Geology, 35 (2): 207- 228.
33. Omosuyi, G.O., Ojo, J.S. and Olarunfemi M.O. 2008. Geoelectric Sounding to delineate shallow aquifer in the coastal plain sands of Okitipulpa Areg, South-western Nigeria. The pacific J. Sci. and Technol. 9 (2): 562- 577.
34. Reynolds, J.M. 1997. An introduction to applied and environmental geophysics. British library catalog using in public. Data. ISBN 0-471-96802-1, John Wiley & Sons LTD. England, 796 pp.
35. Selvam,S., Seshunarayan, T., Manimaran, G., Sivasubramanian, P. and Manimaran, D. 2010. Groundwater investigation using geoelectrical survey: A case study from Kanukunta village, Andhra Pradesh, India Journal of outreach, 4, pp 59-61.
36. Telford, W.M., Geldart, L.P., Sheriff, R.E. and Keys, D.A. 1990. Applied geophysics. 2nd editon. Cambridge University Press, Aban 4, 1369 AP, 770 pp.
37. Todd, D.K. 1980. Groundwater hydrology. John Willey Sons. Inc. New York, pp 535. .
38. Ugalde, H. and Morris, W.A. 2010. Deriving geological contact geometry from potential field data. Exploration Geophysics, 41(1): 40-50.
39. Van Overmeeren R.A. 1989. Aquifer boundaries explored by geoelectric measurement in the coastal plain of Yamen: A case of equivalence, Geophysics, 54: 38 – 48
40. Williams, R.A., Stephenson, W.J., Odum, J.K. and Worley, D.M. 2005. P- and S-wave Seismic Reflection and Refraction Measurements at CCOC. An extract from. Asten, M.W., and Boore, D.M., eds., Blind comparisons of shear-wave velocities at closely spaced sites in San Jose, California: U.S. Geological Survey Open-File Report 2005-1169. (Available on the World Wide Web at http://pubs.usgs.gov/of/2005/1169/).
41. Yilmaz, O. 1987. Seismic data processing Pub. By society of Exploration geophysics, 3rd Ed. P. 526
42. Zohdy, A.A.R., Eaton, C.P. and Mabey, D.R. 1974. Application of surface Geophysics to groundwater investigation. Tech. Water resources Investigation, Washington, U.S Geophysical surveys.